Effects of Processing on Microstructure and Properties of Ti-Ta Alloys

by

Bryan Gortikov

Submitted to the Department of Materials Science and Engineering
in partial fulfillment of the requirements for the degree of

Bachelor of Science

at the

MASSACHUSETTS INSTITUTE OF TECHNOLOGY

[June 2008]
May 2008

Author.....
Department of Materials Science and Engineering
May 16, 2008

Certified by.....
Samuel M. Allen
POSCO Professor of Physical Metallurgy
Thesis Supervisor

Accepted by.....
Caroline A. Ross
Chair of the Undergraduate Committee

Effects of Processing on Microstructure and Properties of Ti-Ta Alloys

by

Bryan Gortikov

Submitted to the Department of Materials Science and Engineering
On May 17, 2008, in partial fulfillment of the
requirements for the degree of
Bachelor of Science

Abstract

Titanium-Tantalum shape memory materials have widespread potential in biomedical applications due to their high degree of biocompatibility, favorable mechanical properties, high corrosion resistance and the possibility of exhibiting shape memory behavior[5, 6, 9]. However, this system faces difficulties in processing due to the slow diffusion of Ta, with a melting point of 3269 K, and the sensitivity of shape memory materials on composition and processing history[8, 9]. Dynamet Technology, Inc. has engineered a process in which these difficulties are overcome via powder metallurgy techniques, and the objective of this work was to characterize and explore the relationship between Dynamet's processing steps and the microstructure and properties of the Ti – 30 wt % Ta system[5]. Energy-dispersive x-ray analysis was used to quantify compositional gradients to verify homogeneity. Room temperature and high temperature x-ray diffractometry was used to identify phases present at temperatures ranging from room temperature up to 750 °C. Hot extrusion without further heat treatment was found to be insufficient to produce a homogenous, fully dense alloy. Elongation, an indicator of potential shape memory behavior, was shown to increase with increased martensite phase fraction, which is thought to be dependent on cooling rate from above the austenite phase transformation starting temperature, A_f. Finally, a phase transformation, likely that of martensite into beta-Ti, was verified to exist between 400 – 600 °C.

Table of Contents

Table of Figures

1. Introduction

Since their discovery in 1961, shape memory alloys have gained attention for their unique properties[1]. Even after severe deformation, shape memory alloys (SMAs) are capable of returning to ("remembering") their original geometry through a solid-state diffusionless phase transformation[2]. SMAs are mixtures of martensitic and austenitic phases that transform into one another via thermal or mechanical means[2]. This shape memory effect lends itself it a variety of applications. SMAs have been used as anti-scalding devices in water faucets and shower heads as active materials that can restrict the flow of liquid upon reaching a particular temperature[1]. Currently, SMAs are extensively used in biomedical applications. Orthodontic wires, catheters, and intravascular stents are particular examples of medical devices that benefit from the shape memory effect in these unique alloys.

Titanium alloys see wide use in biomedical applications. Titanium (Ti) alloys such as Ti-6Al-4V, a structural material, and TiNi (Nitinol), a widely used shape memory alloy, have a long history of successful use in medical implants, but both are plagued by a variety of problems that make them an unfavorable choice for use within the body. For example, Ti-6Al-4V has an elastic modulus that is significantly higher than that of bone; this causes implants to reduce load on the bone and this poses a risk of bone resorption. V and Al are cytotoxic and dangerous if they become absorbed in the body. Most importantly for shape-memory applications, a portion of the population is hypersensitive to Ni; studies in Europe show 15% of the female population to be allergic to Ni[3]. Due to its low corrosion resistance, in vivo failure of TiNi-based implants causes dangerous leakage of Ni into the body. Thus, there is an interest in the development of Ni-free Ti-based shape memory alloys.

Shape memory behavior has been demonstrated in a number of Ni-free Ti alloy systems, but the Ti-Ta system is of particular interest for orthopaedic and orthodontic applications[4]. The shape memory effect is made possible by the transition between beta-phase Ti and martensite. Binary Ti-Ta alloys are particularly amenable to heat treatment, as a fully beta structure can be achieved at room temperature[5]. Previous work on Ti-Ta alloys of composition ranging from 20 – 60 wt% Ta has shown that the Ti-30 wt% Ta alloy provides a promising combination of mechanical properties, elongation, and homogeneity[6]. The elastic modulus of Ti-30Ta is closer to that of bone than other Ti alloys; this would help minimize stress shielding and allow bone to carry more of its normal load, mitigating the problem of resorption[5]. Ti-Ta alloys would be at least as biocompatible as Ti, as Ta is considered inert in the body[5]. Finally, the Ta stabilizes the beta-phase near room temperature, making martensitic transformation possible and potentially enabling shape memory behavior.

2. Objective

The objective of this project was to determine both qualitatively and quantitatively the effects of processing history on the microstructure and mechanical properties of the Ti – 30wt% Ta alloy. A scanning electron microscope (SEM) was used to perform energy dispersive x-ray analysis (EDX) to determine specimen composition over a large area. Series of smaller area scans were used to measure compositional variation over short distances. X-ray diffractometry (XRD) was used to determine crystal structure and phase fraction of all phases present at room temperature in Ti- 30 wt % Ta, and high temperature XRD was used to document phase transformations that occur on heating to 750 °C.

3. Experimental Method

3.1 Ti-Ta Alloy:

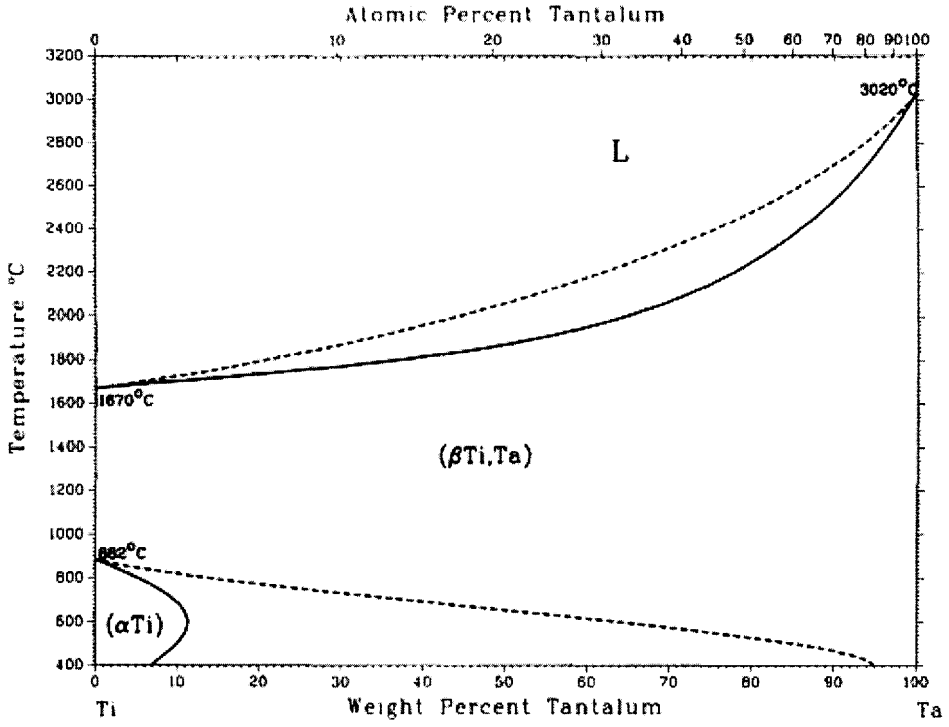

Figure 1. Ti-Ta binary phase diagram. Source: ASM Handbook

Table 5. List of samples, processing methods, and deformation data. Data provided by Dynamet Technology, Inc.

Sample	Processing	Area Reduction:	Elongation:
As-extruded S/N2	Canned, Sintered, Extruded	-	-
Deformed S/N2	Canned, Sintered, Extruded	19%	14%
As-extruded S/N4	Canned, Sintered, Extruded	-	-
Deformed S/N4	Canned, Sintered, Extruded	58%	24%
As-extruded S/N2B	CIP, Sintered, Extruded, HT	-	-

Ti-Ta alloy samples, listed in Table 1, were created via powder metallurgy techniques by Dynamet Technology, Inc. In this process, elemental powders of controlled morphology and particle size were blended in a ratio of Ti – 30 wt% Ta. Tantalum powder size was reported to be less than 44 micron, and the titanium powder size was reported to be approximately 100

micron. As-extruded S/N2B was first cold isostatically pressed, while powders in all other samples were canned before sintering. All samples were vacuum sintered at 2100°F for 24 hours at 5 x 10^{-4}-10^{-6} Torr, cooled no faster than 20 °F per minute to 1700 °F, then argon cooled to 200°F. All samples were extruded from approximately 2.8" diameter x 9" long billets to 1"diameter bars at 1900°F. The as-extruded sample S/N2B underwent additional heat treatment to promote homogenization, but details of this process were not revealed by Dynamet.

According to the Ti-Ta phase diagram, there exist two equilibrium solid-state phases of Ti-Ta. Alpha-Ti is a Ta-poor phase with a hexagonal close packed crystal structure (Figure 1). The solubility limit of Ta in the alpha phase is approximately 12 wt % Ta at 600 °C. Beta-Ti is the Ta-rich phase in the Ti-Ta system and has a body centered cubic structure. There also exists a non-equilibrium martensitic phase with an orthorhombic structure.

3.2 Metallographic Sample Preparation

Table 6. Tensile testing data for two of three batches from which samples were provided. Data provided by Dynamet Technology, Inc.

Serial No.	Ultimate Tensile Strength (msi)	Elongation (%)	Reduction of Area (%)	Youngs Modulus (msi)
S/N2	134	14	19	13.24
S/N4	109	24	58	10.33

All samples were cut from tensile test specimens using a low speed diamond saw. As-extruded samples were cut from the threaded region of the tensile specimen, while deformed samples were cut from within 2 mm of the fracture surface, within the necked region. Deformation data for these samples are listed in Table 2. For all experiments, samples were mounted in Struers Multifast Green Bakelite with the extrusion direction normal to the sample surface. The Bakelite solidification process involved a four minute ramp up to and a ten minute hold at approximately

150°C followed by a 4 minute cooling period. Samples were then polished to a final surface roughness of 3 microns using diamond paste.

To observe the microstructure of the Ti-30 wt% Ta alloy, some samples were etched before observation via optical and SEM imaging techniques. All etched samples were treated with Kroll's etchant, composed of 0.5 mL HF, 1.0 mL HNO_3, and 200 mL H_2O. As-extruded S/N2 was etched for a total of 60 seconds (2 sets of 30 seconds), and deformed S/N2 was etched for a total of 90 seconds (40 seconds followed by 50 seconds). It should be noted that extended etching period of deformed S/N2 was due to a timing error and was unintended.

3.3 Energy-Dispersive X-ray Analysis

A Leo VP438 Scanning Electron Microscope was used to gather elemental data via energy-dispersive x-ray analysis. The x-ray detector, an X-ray Optics Model 31002, used a Lithium-drifted silicon detector with 128 eV resolution and a 10 mm crystal. The signal was processed using an IXRF Model 500 Digital Pulse processor and analyzed using EDS 2004 software.

3.4 X-ray Diffractometry

X-ray diffraction data was gathered using a Bruker D8 Discover diffractometer. This instrument was used because to its ability to resolve and account for effects of crystallographic texture via the two-dimensional General Area Diffraction Detector System (GADDS). The detector placed 150mm from the sample and collected in 25°2θ segments. Data is collected simultaneously along both the 2θ axis and approximately 25° of the c axes. Two dimensional data was summed along the chi axis to produce intensity plots, and individual frames were amalgamated using Jade MDI Software.

Table 7. List of high temperature XRD measurement temperatures of as-extruded S/N2B. All heating and cooling was done at a rate of 50°C/minute.

Measurement Temperature (deg C)	Wait Time (min)
25	-
100	5
300	5
400	5
600	0
750	0
25	Overnight

In the high temperature XRD measurement of as-extruded S/N2B, specimens were heated using an Anton Paar DHS900 dome furnace. This instrument is capable of reaching 900°C and consists of a hot plate, an insulating polymer cap, and a cooling rod used as a means of air-cooling the dome. Rather than being mounted in Bakelite, the sample was placed directly on the hot plate. The sample was subsequently heated to 750°C and cooled back down room temperature, with measurements taken at specific intervals, as shown in Table 3. The degree of rotational freedom of the sample was restricted by a cooling tube, and as a result a "comprehensive" scan similar to those done at room temperature could not be performed.

4. Results & Analysis

4.1 Compositional Analysis

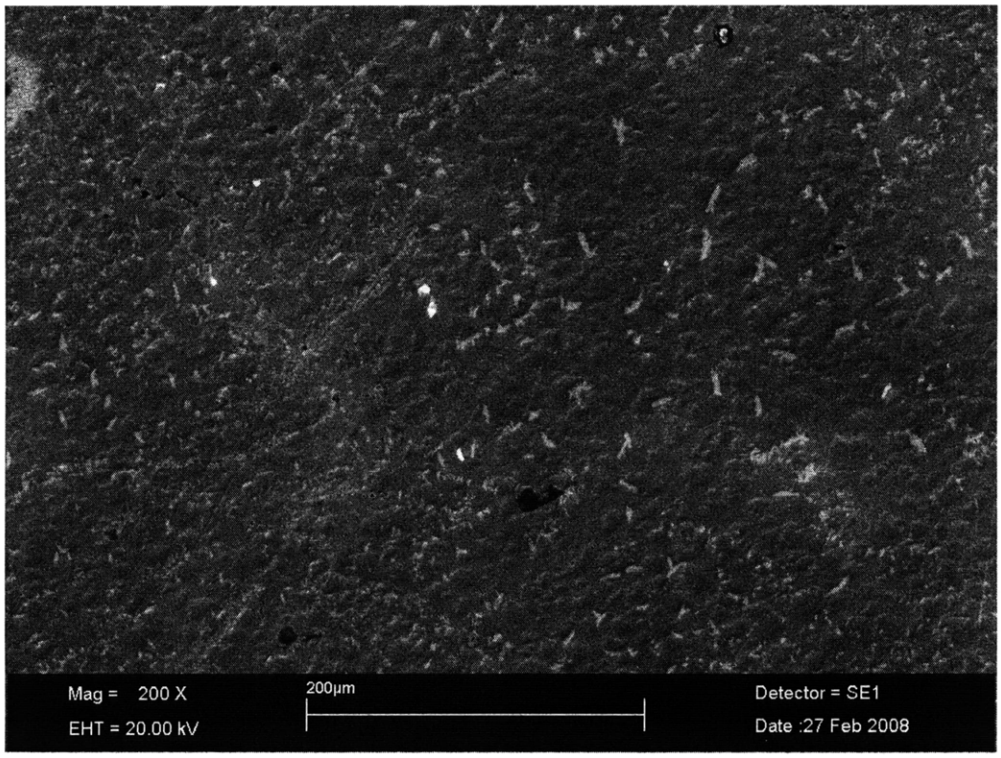

Elt.	Line	Intensity (c/s)	Error 2-sig	Atomic %	Conc		
Ti	Ka	740.47	5.442	86.804	63.506	wt.%	
Ta	La	35.11	1.185	13.196	36.494	wt.%	
				100.000	100.000	wt.%	Total

Figure 2. Secondary Electron SEM image of as-extruded S/N2 sample and its corresponding EDX compositional analysis. Compositional data was averaged over the entire visible area.

Despite a reported composition of Ti-30wt% Ta, EDX results averaged over an approximately 500 um x 500 um area of as-extruded S/N2 show a measured composition of Ti - 36 wt% Ta +/- 3.6% (Figure 2). Despite being taken at the relatively low magnification of 500x, EDX

measurements at lower magnifications may generate results that more closely match the reported composition values. As previously reported, this preparation of Ti-Ta binary alloys leads to greater inhomogeneity with increasing Ta[6]. Ti-Ta interdiffusivity has since been shown to decrease with Ta concentration in a specimen that had been canned, consolidated and annealed[8]. Even at low magnification, lighter, Ta-rich regions are clearly observable by SEM. It has been reported that these lighter particles have a high aspect ratio; when the section plane is parallel to the extrusion axis, they appear long and thin.

a)

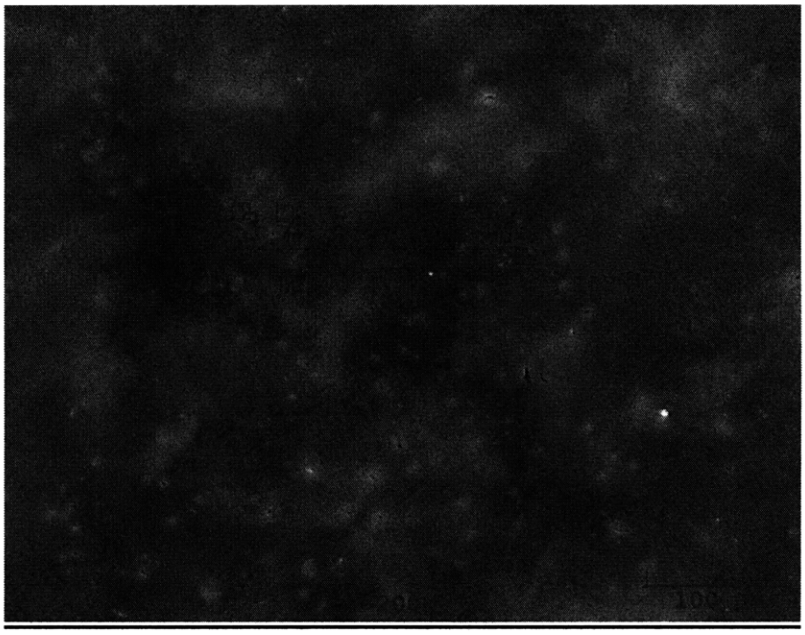

b)

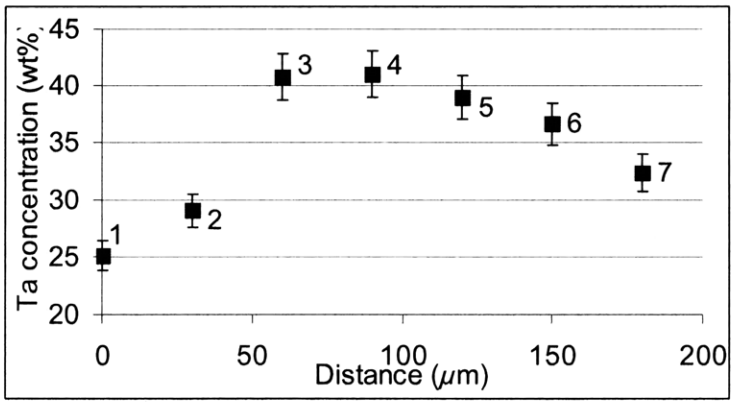

Figure 3. a) Secondary Electron SEM image of an as-extruded S/N4 sample with annotated area scan locations. b) Ta concentration (in wt %) vs. distance, with data points corresponding to annotated locations in Figure 2a.

Figure 3 shows a series of small area scans along a line of varying contrast (dark-light-dark). Despite a nominal composition of 30 wt% Ta, Ta concentrations were found vary from as low as 25 wt% and as high as 42 wt% over a distance of 100 um. Dynamet's processing method creates a high-density alloy, but one that includes some residual porosity and compositional inhomogeneity[8]. Due to the very high melting point of tantalum (3000°C) and the large difference in atomic radius between Ti (T_{mp} = 1668°C) and Ta, interdiffusion between Ti and Ta is extremely slow at Ti sintering temperatures. This inhomogeneity is believed to be the cause of difficulty when attempting to use Differential Scanning Calorimetry (DSC) to verify the martensitic phase transformation in Ti-30Ta. The temperature at which this diffusionless transformation occurs is dependent on composition (Figure 1). The presence of a continuous distribution of concentrations between, at least, 25-42 wt% Ta causes a similarly continuous distribution of phase transformation temperatures, which is believed to obscure the distinct peak that would be expected in heat flow vs. temperature plots gathered using DSC. This difficult may, however, also have been due to the equipment's inability to reach high enough temperatures to identify phase transformations.

Since the finding of these results, Dynamet has supplied us with a specimen that underwent altered processing in order to ensure increased homogeneity (sample S/N2B). Rather than being canned and sintered, the powder mixture was cold isostatically pressed before sintering and extrusion. Following extrusion, however, the alloy was heat treated to increase Ta diffusion. Preliminary results show nearly a 20% increase in elongation compared with as-extruded samples, but due to time constraints metallography and composition scans of this material will be accomplished in a later study.

4.2 Microstructure

a)

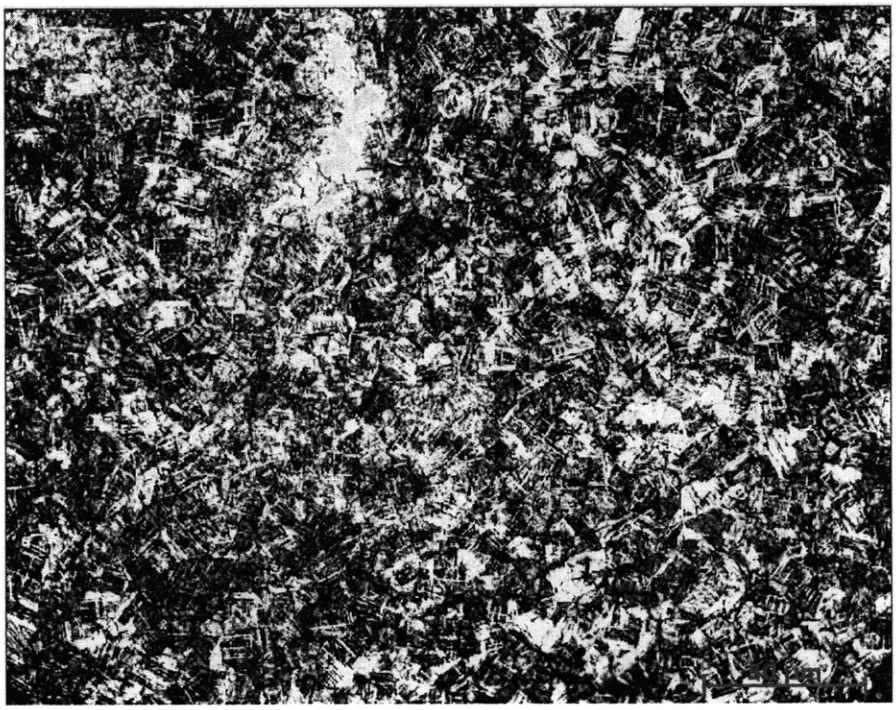

b)

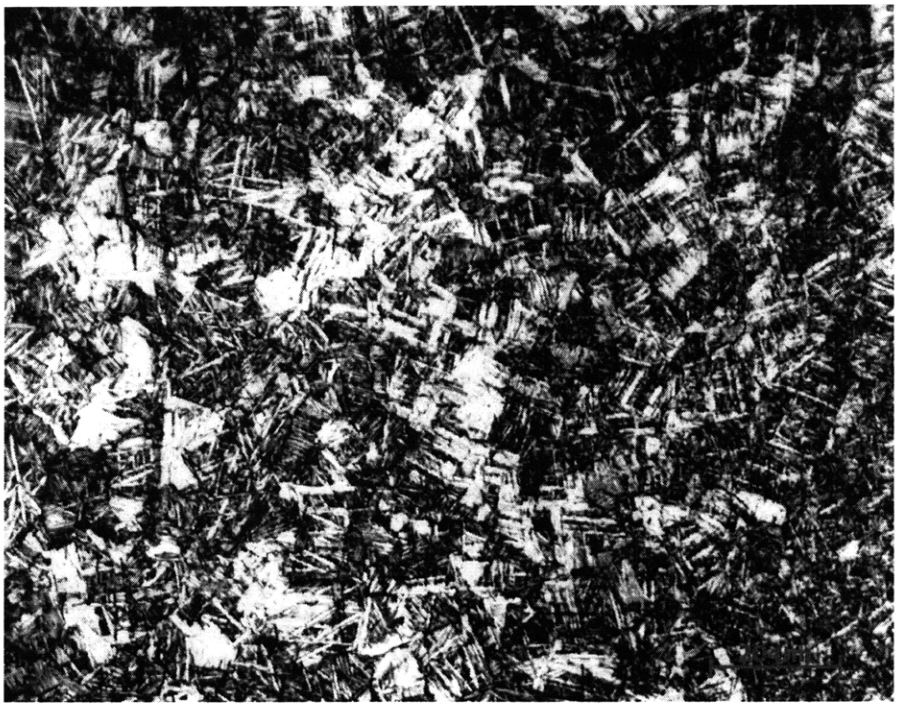

Figure 4. Optical images of Ti-30 wt%Ta. a) As-extruded S/N2 at 50x. b) As-extruded S/N2 at 100x.

Figure 4 shows optical microscope images of the microstructure of deformed and as-extruded samples at 50x and 100x. Though it cannot be confirmed, the size, shape and contrast of the lighter areas lead us to believe that they are beta-Ti. Clusters of beta-Ti dispersed within a plate-like microstructure consisting of layers of alpha-Ti and beta-Ti can be seen in Figure 4b.

a)

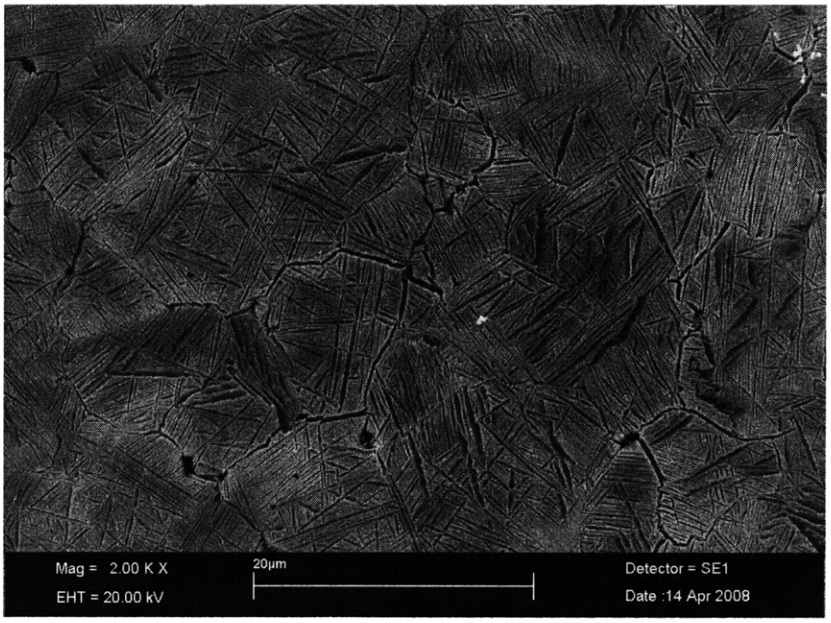

b)

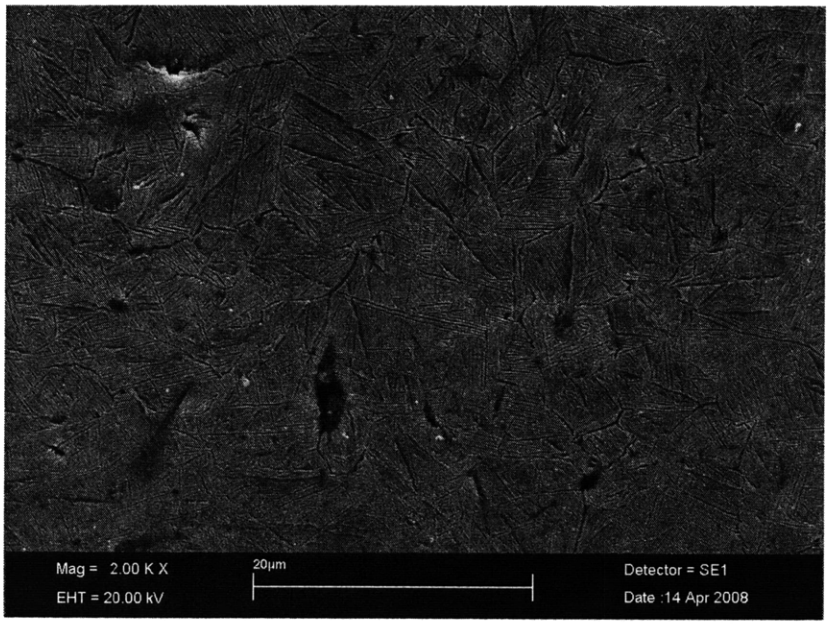

c)

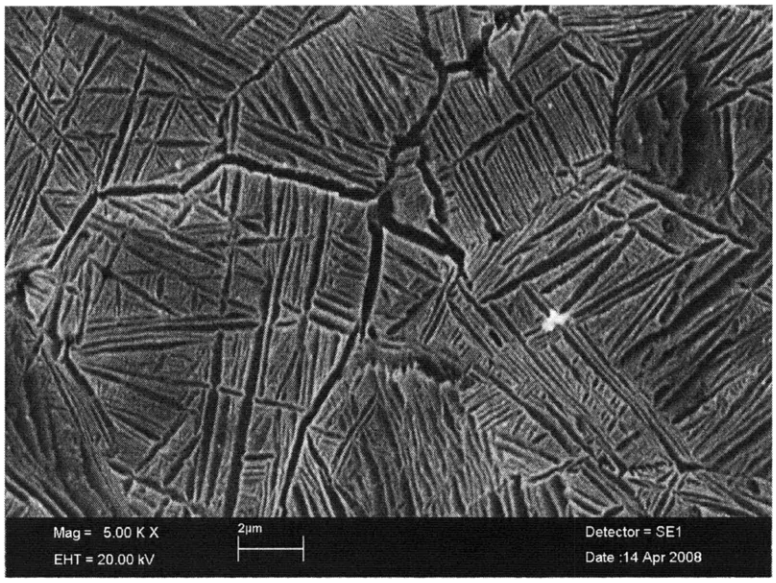

d)

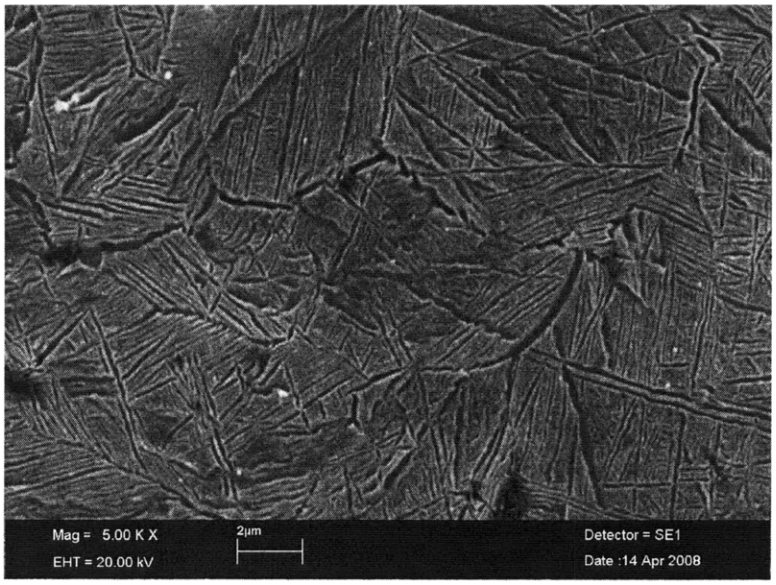

Figure 5. Secondary Electron SEM Images of as-extruded and deformed S/N2 at various magnifications. a) As-extruded at 2000x. b) Deformed at 2000x. c) As-extruded at 5000x. d) Deformed at 5000x.

A fine, layered structure typical of alpha-Ti can be seen in secondary electron SEM images in Figure 5. More pronounced features separating regions containing parallel plates oriented in different directions are present and presumably are grain boundaries. In both samples, grain size appears to be on the order of 20 µm. The original particle sizes reported by Dynamet were 44

μm and 100 μm for Ta and Ti, respectively. At an extrusion ratio of approximately 2.8:1, these values suggest that the grain structure is a result of the original particle size, arrangement and morphology. Despite our expectation of crystal variant alignment upon deformation, the features in these images appear to be arranged randomly. However the contrast of the image as well as the number of features prevent of from forming a definitive conclusion.

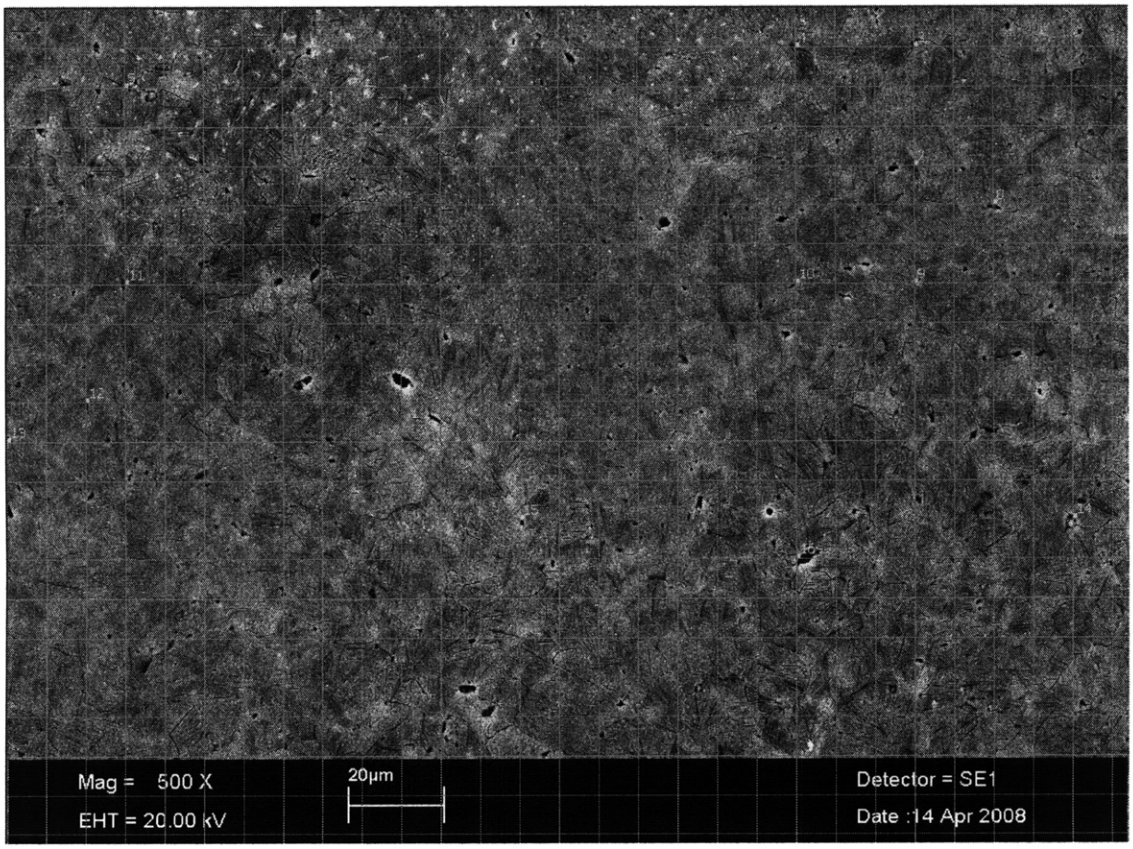

Figure 6. Secondary electron SEM image of as-extruded Ti-30 wt% Ta, serial number S/N2 at 500x. A superposed 29 x 19 line grid was used to determine pore fraction of 2.9%.

One striking feature of these images is the porosity of the alloy. A 29 x 19 line grid was superposed over a secondary electron image of as-extruded S/N2 (Figure 6). By dividing the number of grid intersections that overlap a pore by the total number of intersections, an estimate of overall pore fraction can be determined. Using the image in Figure 6, an overall pore fraction

of 2.9% was calculated. In order to account for variations in local pore density, the image was taken at 500x zoom, the lowest magnification at which pores could be resolved. The high concentration of pores is a direct result of lack of sufficient thermomechanical treatment to obtain a 100% dense material. The pores exist mainly on what appear to be grain boundaries, confirming our hypothesis that diffusion between powder granules during processing was incomplete. The presence of pores degrades the mechanical properties of the alloy, but Dynamet has begun to include a final heat treatment in order to remove pores and create a 100% dense material.

4.3 XRD

4.3.1 Comparison of similarly processed samples S/N 2 vs. S/N 4

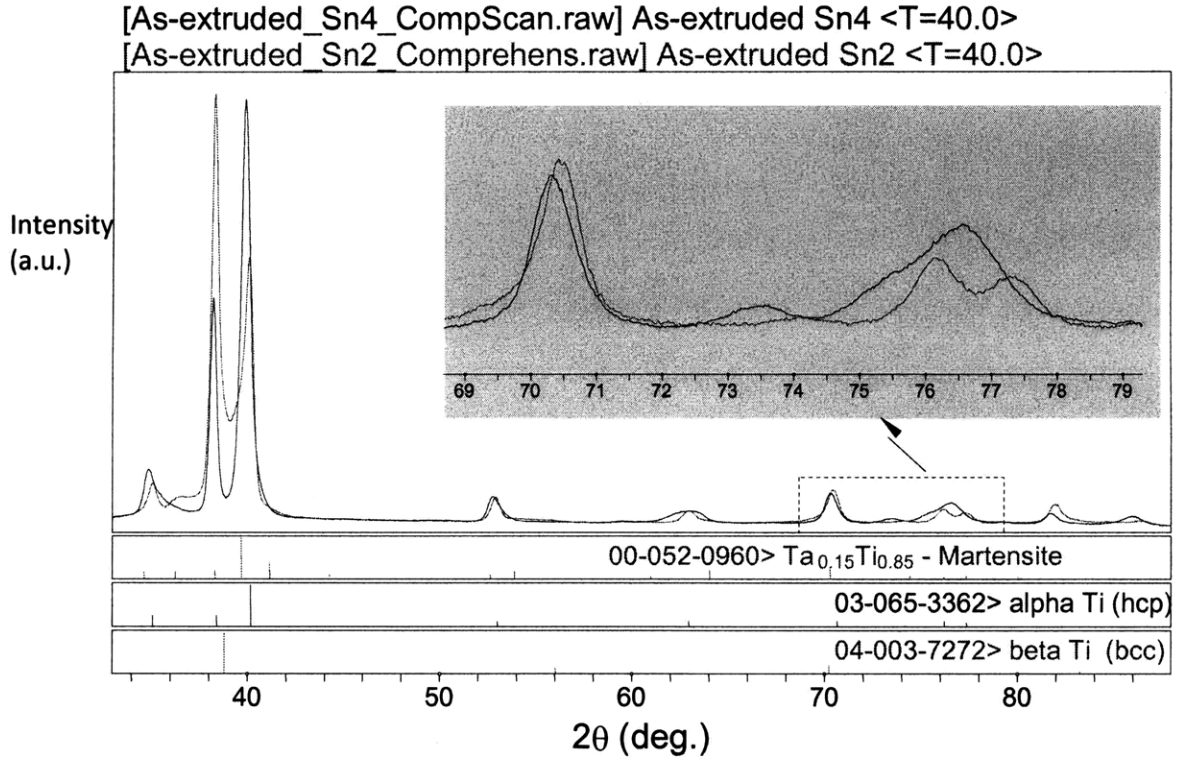

Figure 7. XRD diffraction data of as-extruded S/N 2 and S/N 4.

Figure 7 illuminates the differences in crystal structure between as-extruded samples of S/N 2 and S/N 4. A comparison of mechanical properties of the two samples can be found in Table 2. Despite a similar processing history, samples S/N 2 and S/N 4 have very different mechanical properties. The most striking difference is the significantly higher elongation in S/N 4. Intensity versus diffraction angle data shows both samples contain alpha-Ti, beta-Ti and orthorhombic martensite. S/N 2 has a higher beta phase fraction when compared to S/N 4, which is almost entirely composed of martensite. This analysis matches with the previously described explanation of shape memory behavior. Upon deformation, the martensite crystal variants may reorient along a preferred crystallographic axis. The extent to which a shape memory alloy can be deformed and subsequently recovered is dependent the fraction of martensite in the original material. Upon heating, martensite transforms into body-centered cubic beta-Ti, but the presence of beta phase before deformation hinders shape memory behavior and could account for the lower elongation of S/N 2. These results may arise from small variations in Dynamet's processing methods (i.e. canning rather than cold isostatically press, no heat treatment) used to create S/N2 and S/N4.

4.3.2 Comparison of as-extruded vs. deformed samples

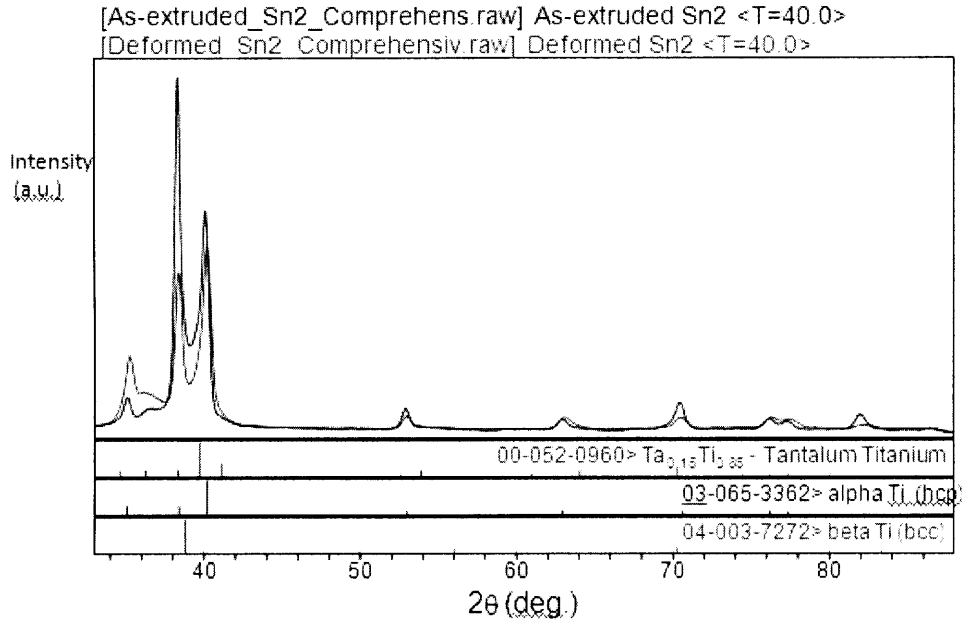

a)

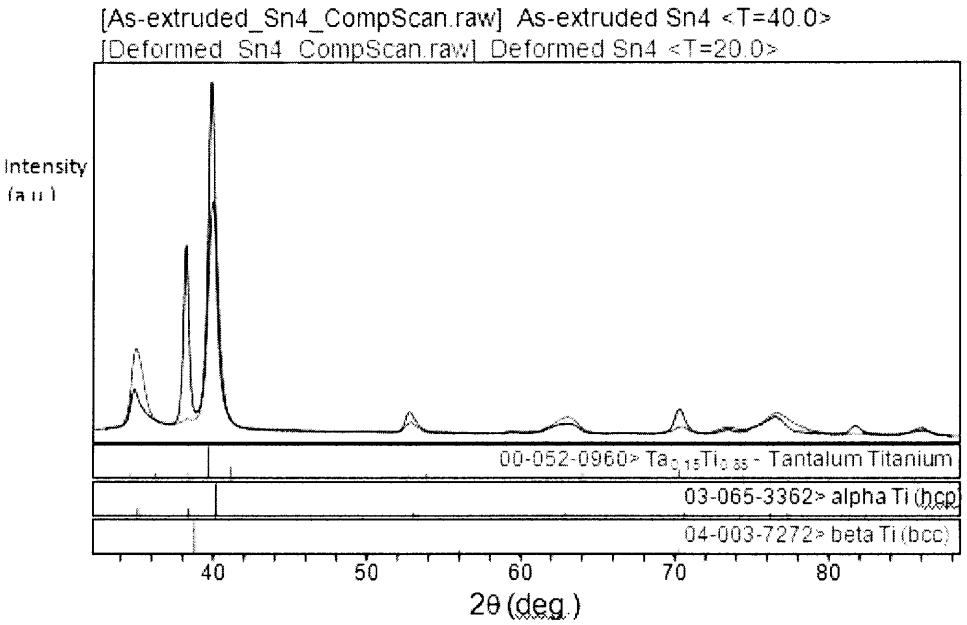

b)

Figure 8. XRD diffraction data of as-extruded and deformed samples of Ti- 30 wt% Ta. a) S/N2. b) S/N4.

Figure 8 shows differences in crystal structure between as-extruded and deformed samples of S/N2 and S/N 4. Upon deformation there is an apparent increase in martensite phase fraction. This is possibly due to the martensite crystal grains orienting in a direction that produces greater martensite peak signal. Grain alignment may also be the reason that the (002) and (004) peaks disappear upon deformation of S/N 4 (Figure 8b). However, this may also arise from a real increase in martensite fraction; Zheng et. al. found that upon straining the 50Ni-48Ti-2Fe shape memory alloy via nanoindentation techniques, a strain-induced martensitic phase could be identified by transmission electron microscropy[7]. Similar processes may also occur in the Ti- 30 wt % Ta shape memory alloy.

Table 8. Observed vs. reference card lattice parameters for orthorhombic martensitic Ti-Ta

	a	b	c
Reference:	3.038	4.957	4.686
Observed:	2.99	5.02	4.70
Difference:	-1.6%	1.3%	0.3%

There exists a small mismatch between observed peak locations of S/N 4 and powder diffraction file reference locations in Figure8b, but this may be attributable to lattice distortion due to a compositional gradient either in martensite or in beta-Ti. Table 4 shows a comparison of reference lattice parameters and observed lattice parameters for the martensitic phase in as-extruded S/N 4.

4.3.3 Verification of the martensitic phase transformation

a)

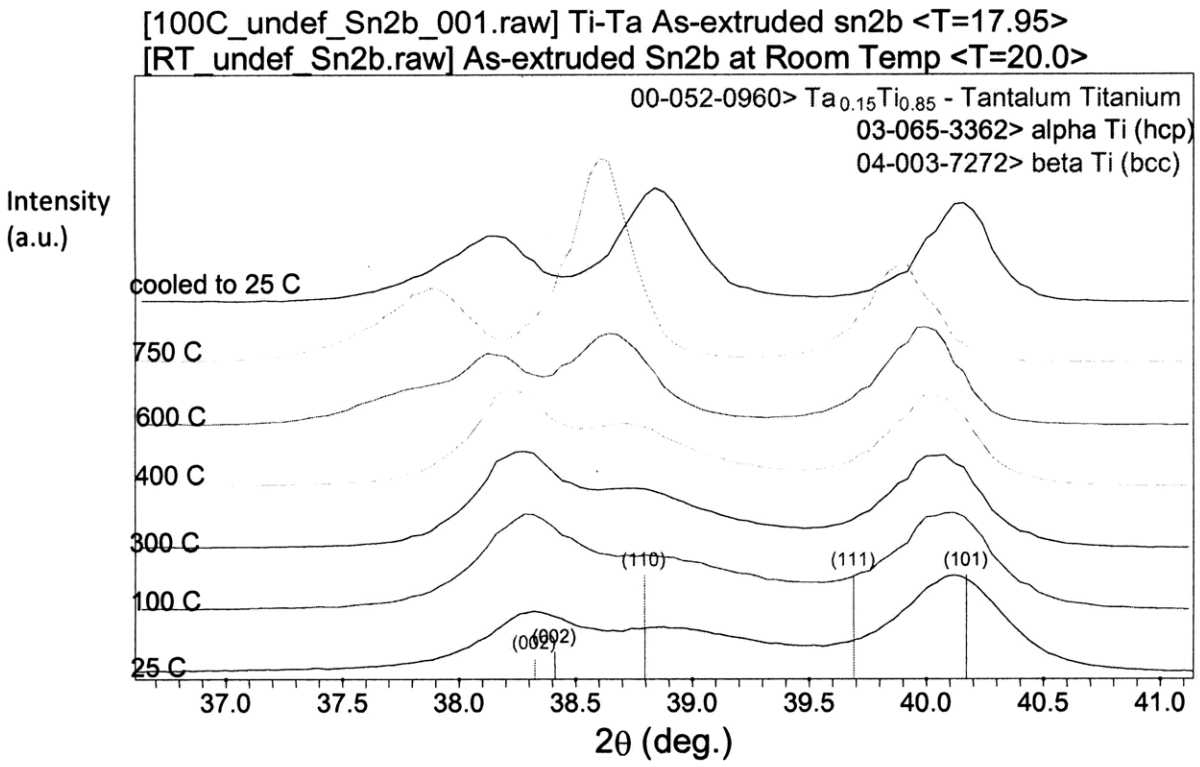

b)

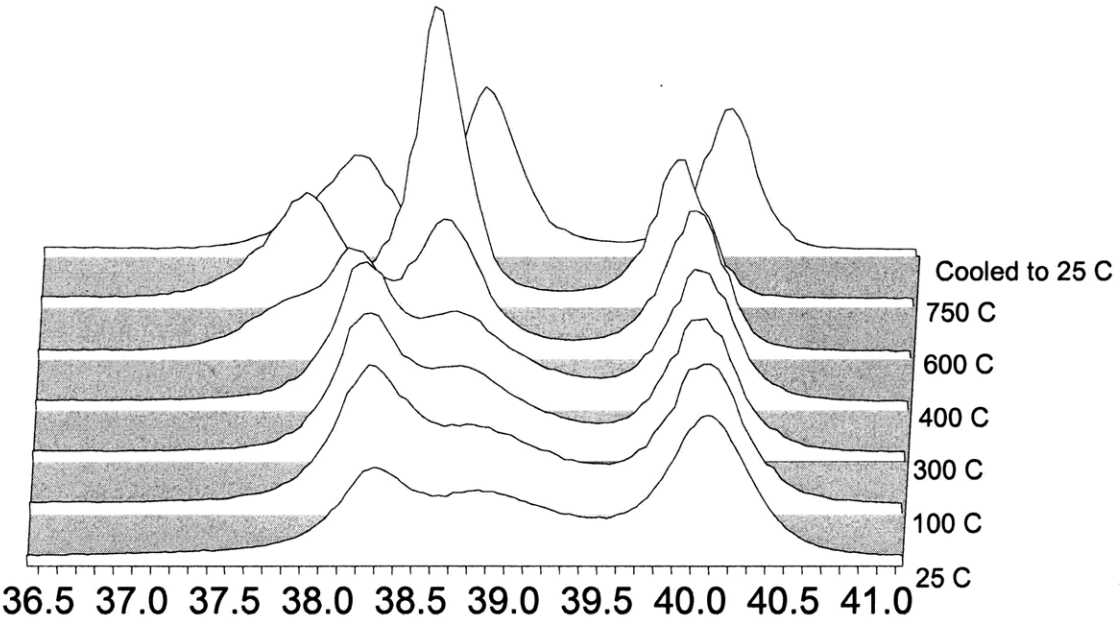

Figure 9. XRD diffraction data for homogenized Ti-30 wt% Ta. Samples were measured according to data from Table 3. a) 2D plot. b) 3D plot.

Originally, differential scanning calorimetry was attempted to verify the shape memory enabling transformation of martensite into austenite (beta-Ti) above a particular temperature, the austenite phase transformation finishing temperature (A_f). However, the compositional variations of the as-extruded samples are likely to have obscured the expected sharp peak in heat flow vs. temperature plots. Instead, high temperature XRD scans were used to verify a change in crystal structure at discrete intervals from room temperature to 750^{O}C (Figure 9). At 300^{O}C, the beta-Ti (110) peak begins to sharpen possibly due to an attenuation of compositional variations. Upon heating to 600^{O}C, the beta-Ti (110) peak becomes dominant, perhaps signaling the start of the diffusionless transformation from martensite to beta or a diffusional transformation from alpha to beta. A shoulder begins to form on the peak near 2θ of 30^{O}. By 750°C, the martensite has clearly transformed into beta-Ti. Though the data are insufficient to determine the exact austenite finishing temperature, the austenite starting temperature is likely between 400-600°C. Upon transformation, we notice the formation of a low-angle peak that does not match powder diffraction files for alpha-Ti or martensite. This peak may be due to a phase transformation within alpha-Ti, although this is not supported by the Ti-Ta binary phase diagram. Due to time constraints, the sample was not allowed to equilibrate at 600°C and 750°C. Combined with the possibility poor thermal contact and the existence of a thermal gradient between the heating stage and the sample, this may have caused the actual temperature of the sample at our 750°C measurement to be lower than measured and perhaps very close to the maximum solubility limit of Ti in the beta phase around 600°C. Ta-rich inhomogeneities in the beta phase would also allow for increased Ta beta phase lattice parameter. A final hypothesis is that the remaining martensite at 750°C has a higher Ta concentration than the original martensite, shifting its peak

to a lower angle. It should be noted that the general tendency of all peaks to shift towards lower 2theta positions is due to thermal expansion.

After the sample was ramped up to 750°C, it was cooled at 50°C/minute to room temperature and allowed to sit overnight. A final scan was taken the next morning at room temperature and is represented in Figure 9 as "cooled to 25C". Peak locations and relative heights differ greatly between measurements at 25°C before and after the high-temperature x-ray scans. In the cooled sample, we see the (002) martensite and alpha-Ti shift to a lower 2theta value. This shift may be due to a lattice constant distortion due to increased Ta concentration in martensite or alpha-Ti upon cooling. The amount of beta-Ti remaining upon cooling to 25°C is surprising; theory dictates beta-Ti should revert back to martensite below its martensite finishing temperature, or M_f. This may be due to the cooling rate; martensite is said to form upon fast cooling to below room temperature[9]. At a cooling rate of 50 °C/min, the metastable martensite phase may not be able to form.

5. Conclusion and Future Work

By EDX analysis and pore counting methods, we have concluded that the canning, sintering, and extrusion process alone is not sufficient to produce a fully dense Ti-30 wt% Ta alloy. According to a Dynamet, the homogenized alloy (S/N2B) is 100% dense, but due to time constraints this was not verified. In future work, verification of Dynamet's claim of 100% density as well as further exploration, including XRD and EDX analysis, of the fully homogenized alloy should be a primary objective.

In comparing XRD data with reported tensile testing data, elongation, has been shown to be dependent on initial presence of martensite. According to shape memory theory, upon elongation, martensite crystal variants rotate to accommodate load, which supports our conclusion. Martensite phase is said to form upon fast cooling to below room temperature[9]. High-temperature XRD data hints at a strong dependence of martensite phase fraction on cooling rate from above the austenite phase transformation finishing temperature. Further investigation on the effect of cooling rate on Ti-Ta alloys is recommended in order to improve Dynamet's process.

Finally, we have verified a phase transformation into beta-Ti starting between 400-600°C. Martensite is likely to be the beta-Ti precursor phase. This temperature is dependent on composition. In the future, Dynamet plans to explore potential shape memory behavior in higher Ta content Ti alloys, which will require similar testing to verify transformation temperatures. Additionally, these alloys should be tested on an apparatus capable of temperatures exceeding 900°C in order to quantify the austenite transformation finishing temperature. This verification

will not only provide quantitative phase transformation data, but may also provide clarity on phases present at lower temperatures.

Bibliography

[1] Kauffman, G, Mayo, I. *Memory Metal. Chem Matters* Oct. 1993: 4-7.

[2] Sinha, A. *Physical Metallurgy Handbook.* McGraw-Hill Companies, 2003

[3] Disegi, J. A., Titanium *Biomaterials for Orthopaedic Trauma Applications*, Conference Proceedings Titanium 2004 – 20th Annual Conference, International Titanium Association, New Orleans.

[4] US Patent 6,027,585, Patterson et al. Titanium-tantalum alloys 2000

[5] Dynamet's SBIR Phase I Research Proposal. December, 2006.

[6] Allen, S et al. *MIT Report for Phase I Dynamet Technologies, Inc. Grant.* December 2006

[7] Zheng, H., et al., *TEM observation of stress-induced martensite after nanoindentation of pseudoelastic* $Ti_{50}Ni_{48}Fe_2$. Acta Materialia, 2008. **58**(9): p 743-746.

[8] Dibbern, J. *Interdiffusivity in Titanium Tantalum Alloys Processed at 1473 K.* Bachelor of Science Thesis, Faculty of Materials Science, Massachusetts Institute of Technology, (June 2007)

[9] Kollerov, M., et. al. *Martensitic Transformations and Shape Memory Effect in Titanium Alloys*. Titanium '95: Science and Technology Conference. 1995.